Research Article GU J Sci, Part A, 13(2): 838-848 (2026) 10.54287/gujsa.1922780

Gazi University
Journal of Science
PART A: ENGINEERING AND INNOVATION
http://dergipark.org.tr/gujsa

Optical Properties of AlGaN/GaN HEMT Structures

Ahmet Kürşat BİLGİLİ[1*] Yunus BAŞ[1] Orkun SARIARSLAN[1] Sabit KORCAK[2] Mustafa Kemal ÖZTÜRK[1,3]

[1] Gazi University, Graduate School of Natural and Applied Sciences, Ankara, Türkiye
[2] Artvin Çoruh University, Department of Energy Systems, Faculty of Engineering, Artvin, Türkiye
[3] Photonics Research Center, Gazi University, Ankara, Türkiye

Keywords

HEMT
AlGaN
MOCVD
Swanepoel
Tauc
Kubelka-Munk

Abstract

This study investigated the optical properties of AlGaN/GaN/sapphire high-electron-mobility transistor (HEMT) structures. The AlGaN/GaN/sapphire HEMT structures were grown by metal-organic chemical vapour deposition (MOCVD). The aim of this study was to determine the optical properties, layer thicknesses, and band gap energies of the buffer layers. The Swanepoel envelope method was employed to calculate the refractive index, layer thickness, absorption coefficient, and extinction coefficient. These parameters were obtained for the transparent region as well as the weak- and medium-absorption regions. The Tauc method, together with the Kubelka–Munk method, was used to determine the optical band gap energy of the AlGaN layer.

Cite

Bilgili, A. K., Baş, Y., Sarıarslan, O., Korcak, S., & Öztürk, M. K. (2026). Optical Properties of AlGaN/GaN HEMT Structures. *GU J Sci, Part A*, *13*(2), 838-848. doi:10.54287/gujsa.1922780

Author ID (ORCID Number)

0000-0003-3420-4936 Ahmet Kürşat BİLGİLİ
0009-0000-5043-3873 Yunus BAŞ
0009-0003-9852-5752 Orkun SARIARSLAN
0000-0003-1140-6391 Sabit KORCAK
0000-0002-8508-5714 Mustafa Kemal ÖZTÜRK

Article Process

Submission Date 03.04.2026
Revision Date 22.04.2026
Accepted Date 09.06.2026
Published Date 30.06.2026

1. INTRODUCTION

In recent years, III–V semiconductors such as As-based AlGaInAs and P-based AlGaInP have been widely used in laser diodes (LDs) and light-emitting diodes (LEDs) because of their superior properties Rajan et al. (2004). However, their application areas remain limited because the band gaps of these semiconductor materials are insufficient for some optoelectronic applications. With advances in technology, III–V nitride semiconductors such as InN (~0.7 eV), GaN (~3.4 eV), and AlN (~6.2 eV) have attracted considerable interest because of their wide band gaps, high electron saturation velocity, strong chemical bonds, high melting temperatures, high thermal conductivity, and high breakdown electric field Onuma et al. (2003). III–V nitride-based semiconductors cover a broad spectral range extending from the ultraviolet to the infrared region Beeler et al. (2013).

*Corresponding Author, e-mail: sunkurt4@gmail.com

Due to these properties, they are widely used in the fabrication of high-power and high-frequency devices, including AlGaN/GaN and InAlN/AlN HEMTs, HEMTs with GaN and AlN buffer layers, Metal–Semiconductor Field-Effect Transistors (MESFETs), Heterostructure Field-Effect Transistors (HFETs), and Junction Field-Effect Transistors (JFETs). GaN exhibits superior characteristics such as high durability, excellent chemical stability, high electron mobility, and high thermal conductivity Pengelly et al. (2012). GaN-based devices can operate under harsh conditions involving high temperatures, high electric fields, and high frequencies. Consequently, GaN-based HEMT structures are particularly suitable for achieving high power densities.

In this study, the optical properties of AlN/AlGaN-based HEMT structures are investigated. Optical transmittance T(λ), optical band gap (Eg), absorption coefficient α(λ), refractive index n(λ), film thickness (d), and reflectance R(λ) spectra are determined by measuring the intensity of light transmitted through and reflected from thin-film layers deposited on a transparent substrate as a function of wavelength. The relationship between the optical constants of the film and wavelength is examined.

The Swanepoel envelope method is employed to determine the film thickness and refractive index. The transmittance spectrum contains a finite number of interference fringes. Rather than analyzing the entire spectrum, the envelope method utilizes the envelope curves passing through the maxima and minima of the interference fringes. The calculation of fundamental optical parameters using the envelope method was first introduced by Swanepoel.

The Kubelka–Munk theory is also used to determine certain optical parameters of the material. With this method, the relationship between reflection and absorption can be evaluated for specific layers of the device.

Swanepoel envelope method is a photometric characterization method to determine optic constants such as, refractive index, absorption coefficient. Its application only needs transmission spectra. It depends on the interference fringes on envelope curves which are gained by using special softwares.

Tauc method is a graphical method to determine forbidden energy band gap of crystal semiconductors. It uses optical absorption spectra. Relation between absorption coefficient and photon energy is used to obtain the necessary plot. Forbidden energy band gap is gained by x-axis intercept of linear part of this plot.

Kubelka- Munk theory is a model for determining optic properties of diffractive layers such as reflectance and absorption. It determines the optic behavior of sample by using absorption and reflectance of light in sample. It is used for calculating forbidden energy band gap of semiconductors.

2. MATERIAL AND METHOD

AlN and AlGaN layers are grown on a c-oriented sapphire substrate using the MOCVD method. Trimethylgallium (TMGa), trimethylaluminum (TMAl), ammonia (NH_3), aluminum (Al), and nitrogen (N) are used as source materials, while H_2 gas is used as the carrier gas. The TMAl/TMGa flux ratio is approximately between 15% and 25%. TMGa, TMAl and NH_3 are seperated into Ga, Al and N. This seperation is made in MOCVD reactor (Aixron 200/4 HT-S) under low pressure and at low temperature. Transfer of these sources are made with high temperature H_2 carrier gas. Prior to the growth of the epitaxial film, the sapphire substrate is annealed at 1100 ^{0}C for 10 min to remove impurities from the substrate surface. The AlGaN HEMT devices are referred to as Samples A and B. The structures of Samples A and B are shown in Table 1. GaN layers are grown under 200 mbar constant pressure to prevent high level dislocations. For sample A, LT GaN layer is grown in 2.46 minutes and for sample B in 3.31 minutes. Sample A consists of an AlN nucleation layer and GaN buffer layers grown on a sapphire substrate. For Sample A, a thin AlN nucleation layer is first grown at low temperature, followed by the growth of a thick AlN buffer layer at high temperature.

Table 1. *Diagrams of samples A and B*

Sample A AlGaN on AlN template	**Sample B AlGaN on AlN template**
GaN Cap Layer – 3 nm	GaN Cap Layer – 3 nm
AlGaN Layer – 25 nm	AlGaN Layer – 25 nm
AlN Layer – 1-2 nm	AlN Layer – 1-2 nm
GaN Layer – 5 nm	GaN Layer – 5 nm
InGaN Layer – 1 nm	InGaN Layer – 1 nm
GaN Buffer Layer (5) – 150 nm	GaN Buffer Layer (5) – 150 nm
GaN Buffer Layer (4) – 300 nm	GaN Buffer Layer (4) – 300 nm
GaN Buffer Layer (3) – 110 nm	GaN Buffer Layer (3) – 110 nm
GaN Buffer Layer (2) – 800 nm	GaN Buffer Layer (2) – 800 nm
GaN Buffer Layer (1) – 90 nm	GaN Buffer Layer (1) – 90 nm
HT AlN Buffer Layer – 350 nm	HT AlN Buffer Layer – 520 nm
AlN NL	AlN NL
6H-Al_2O_3 Substrate	6H-Al_2O_3 Substrate

The reason for this procedure is to prevent the cracks in nucleation layer. If this temperature adjustment is not made properly, structural properties of device will deteriorate because of high level defects and lattice mismatch.

For Sample B, the growth conditions are the same as those of Sample A. The only difference is the duration of the high-temperature (HT) AlN buffer layer growth. Even this small difference affects all optical and electrical properties of the device because the structural properties change significantly.

3. RESULTS AND DISCUSSION

Swanepoel method

The thickness, absorption coefficient, and refractive index can be calculated using the Swanepoel envelope method. To apply this method to the AlGaN/GaN/sapphire HEMT structure, transmission spectra are used. Transmission is defined as the ratio of the intensity of transmitted light to that of incident light. During the application of the Swanepoel method, the maximum transmission (TM) and minimum transmission (Tm) values can be determined by applying an envelope function using appropriate software. The fitted curves formed by TM and Tm are used in this method Redko et al. (2019), Swanepoel (1983). The results obtained from this method are in good agreement with those reported in the literature.

The transmission spectrum is obtained by plotting wavelength versus %T. This plot is presented in Figure 1 for Samples A and B. No significant differences are observed in the spectra except for fluctuations in the transmission intensity values. These fluctuations may arise from differences in film thickness. Thickness variations may cause the layers to exhibit semi-transparent window behavior. This situation affects the efficiency of the AlGaN HEMT structure Swanepoel (1983), Mohammad and Morkoç (1996).

The interference fringes observed in the transmission spectra are related to variations in film thickness. The forbidden energy band gap can be determined from the high-energy absorption edge. However, this absorption edge may also be associated with excitons rather than band-to-band transitions corresponding to the band gap.

There are various methods for determining the forbidden energy band gap from measured transmission data. Transmission measurements of the AlGaN/GaN/sapphire structure are performed. With the aid of the optical transmission spectra, the thickness of the transparent region, the thickness of the medium- or low-absorption region, the refractive index, excitation, and

absorption constants can be determined Djurisic et al. (2001). In the equations given in the text, ns denotes the refractive index of the substrate (Al_2O_3).

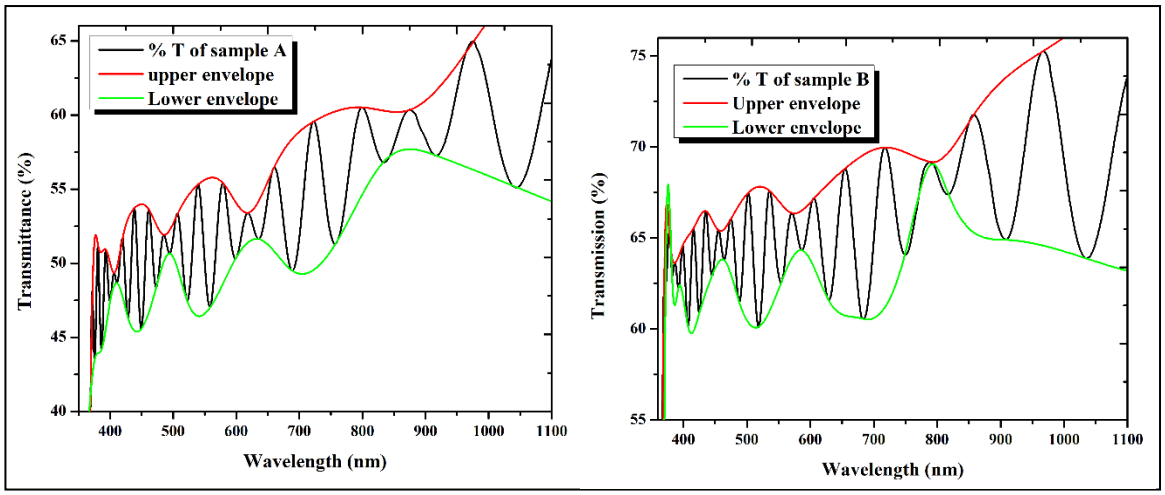

Figure 1. *Transmission spectras and envelopes for Samples A and B*

In Figure 1, the envelope curves can also be observed together with the transmission spectra. These curves are plotted as upper and lower envelopes. TM and Tm can be mathematically modeled as given in Equations (1) and (2).

$$T_M = \frac{Ax}{B - Cx + Dx^2} \tag{1}$$

$$T_m = \frac{Ax}{B + Cx + Dx^2} \tag{2}$$

$$n = [N + (N^2 - {n_s}^2)^{1/2}]^{1/2} \tag{3}$$

$$N = \frac{1}{2}(1 + {n_s}^2) + \frac{2n_s(T_M - T_m)}{T_M T_m} \tag{4}$$

The thickness of the transparent region and that of the medium- or low-absorption region can be determined using Equation (5). In Equation (5), t represents the thickness. The quantity expressed in nanometers (nm) corresponds to the thickness of the transparent and absorption regions.

$$t = \frac{\lambda_1 \lambda_2}{2[n_{(\lambda_1)}\lambda_2 - n_{(\lambda_2)}\lambda_1]} \tag{5}$$

Wavelength versus refractive index plot is demonstrated in Figure 2.

In the samples used, the structures are considered bulk materials consisting of transparent and absorption layers for the incident wavelengths. Therefore, the refractive index values obtained do not correspond to a specific layer. Instead, they represent the transparent and absorption layers as a whole.

The refractive index values for both the transparent region and the low- or medium-absorption region are nearly constant. As expected, the refractive index values of the transparent region are lower than those of the low- or medium-absorption region. This behavior can be explained using the relation n = c/v, where n is the refractive index, c is the speed of light in a vacuum, and v is the speed of light in the medium. The nearly constant refractive index values imply that the samples possess good crystal quality Sakalauskas et al. (2010).

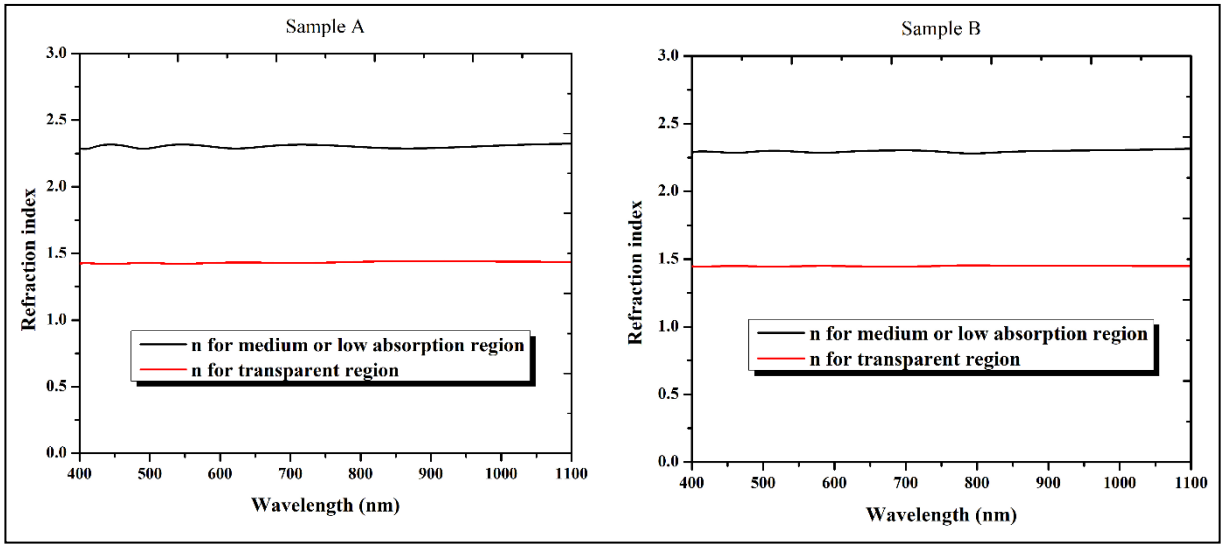

Figure 2. *Refractive index versus wavelength plots for Sample A and B*

The absorption coefficient values in the low- or medium-absorption region are not zero. During the calculation of the absorption coefficient, the parameters x and EM are used in Equations (6) and (7). The absorption coefficient and extinction coefficient are determined using Equations (8) and (9) Romanov et al. (2015). The refractive index, extinction coefficient, absorption coefficient, and thickness values are presented in Table 2.

$$x = \frac{E_M - [{E_M}^2 - (n^2-1)^3(n^2-{n_s}^4)]^{1/2}}{(n-1)^3(n-{n_s}^2)} \tag{6}$$

$$E_M = \frac{8n^2 n_s}{T_M} + (n^2-1)(n^2-{n_s}^2) \tag{7}$$

$$\alpha = \frac{1}{t} ln(\frac{1}{x}) \tag{8}$$

$$k = \frac{\alpha\lambda}{4\pi} \tag{9}$$

In Table 2, "tran." is the abbreviation for transparent. The symbol n denotes the refractive index, while l and w denote low and weak, respectively. The symbols k and α represent the extinction coefficient and absorption coefficient, respectively. The symbol t denotes the thickness. The optical extinction coefficient indicates the extent to which incident light is attenuated within the material.

The absorption coefficient is a measure of the decrease in light intensity as light propagates through the medium.

Table 2. *Optic properties of Samples A and B*

Sample	n (tran)	n l or w	k	α (m^{-1})	t tran (nm)	t l or w (nm)
Sample A	1.30	2.30	$1.1x10^{-3}$	$9.7x10^{-3}$	2454	1591
Sample B	1.40	2.25	$1x10^{-3}$	$9.6x10^{-3}$	2674	1604

Tauc's method

In semiconductor materials, the forbidden energy band gap can be determined using the effect of photon energy on the absorption coefficient. This approach is known as the Tauc method Bilgili et al. (2019). The Tauc method is a widely used technique for determining the forbidden energy band gap from optical absorption spectra Dolgonos et al. (2016). Figure 3 shows the absorption-versus-wavelength plots for Samples A and B. The application of the Tauc method based on the data presented in Figure 3 is illustrated in Figure 4. According to this plot, light is completely absorbed around the visible region. The forbidden energy band gap of AlGaN is determined to be in the range of 2.5–3.0 eV.

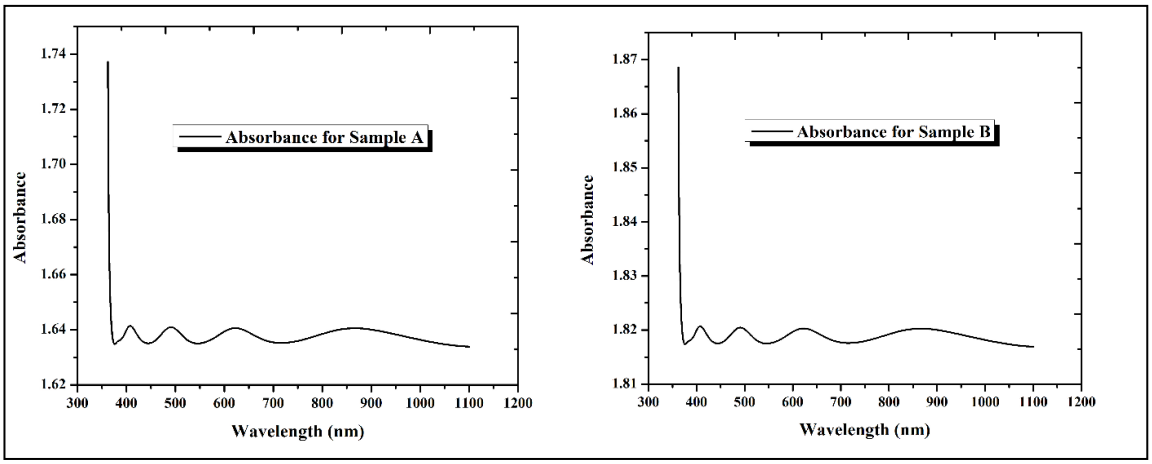

Figure 3. *Absorbance versus wavelength plots for samples A and B*

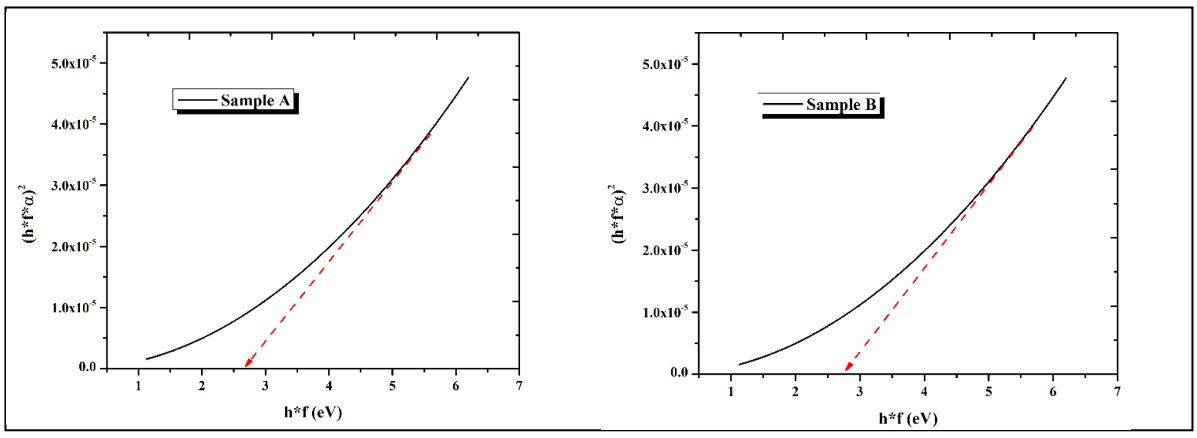

Figure 4. *Demonstration of Tauc's method for samples A and B*

Kubelka-Munk method

The forbidden energy band gap value of AlGaN is calculated again using the Kubelka–Munk model. In this study, the Kubelka–Munk theory is partially applied. The Kubelka–Munk theory is a modeling approach used to describe the behavior of light in absorbing media Alcaraz de la Osa et al. (2019). The application of the Kubelka–Munk method begins with plotting reflectance versus wavelength. The reflectance-versus-wavelength plot is obtained by converting the absorption data into reflectance using Equation (10).

$$R = 1 - \sqrt{Te^{A}} \tag{10}$$

This plot is shown in Figure 5.

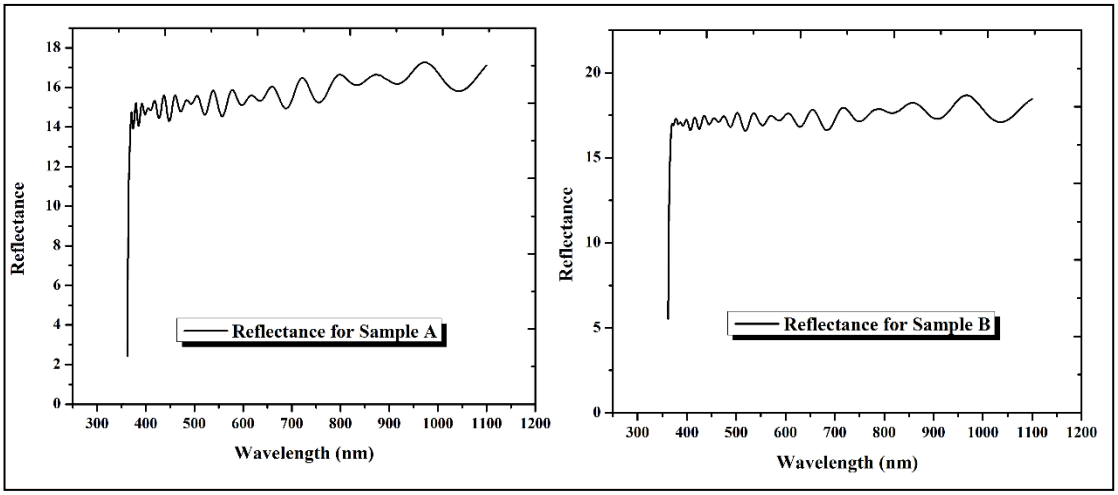

Figure 5. *Reflectance versus wavelength plots for samples A and B*

As the final step, dR/dλ versus wavelength is plotted. The center of the highest peak in this plot provides the wavelength value used to determine the forbidden energy band gap through the relation hc/λ. The dR/dλ versus wavelength plots are shown in Figure 6. These plots represent part of the Kubelka–Munk theory. The center of the highest peak is located at 389 nm for Sample A and 412 nm for Sample B. The corresponding energy values are 3.18 eV and 3.00 eV, respectively.

The Al ratio corresponding to these band gap values is approximately 20%. The lower band gap may result from several factors. For example, Al incorporation during MOCVD growth may be more effective than expected, although measurement errors may also contribute. In addition, alloy disorder, such as inhomogeneous Al distribution or Ga-rich regions, may affect the band gap. Another possible reason is band tailing arising from defects and disorder. Furthermore, strain effects resulting from lattice mismatch may also influence the band gap. Tensile strain in the

structure decreases the band gap. High doping levels may also reduce the band gap. In addition, high growth temperatures may lead to a decrease in the band gap.

Since the wavelength is known, the corresponding energy value can be readily calculated using the relation given by Inbaraj and Prince (2018). It is observed that the forbidden energy band gap values obtained from the Tauc and Kubelka–Munk methods are in good agreement with each other. According to data and results gained by calculations and measurements, band gap values, some optical coefficients are determined in good accordance with literature given in references section.

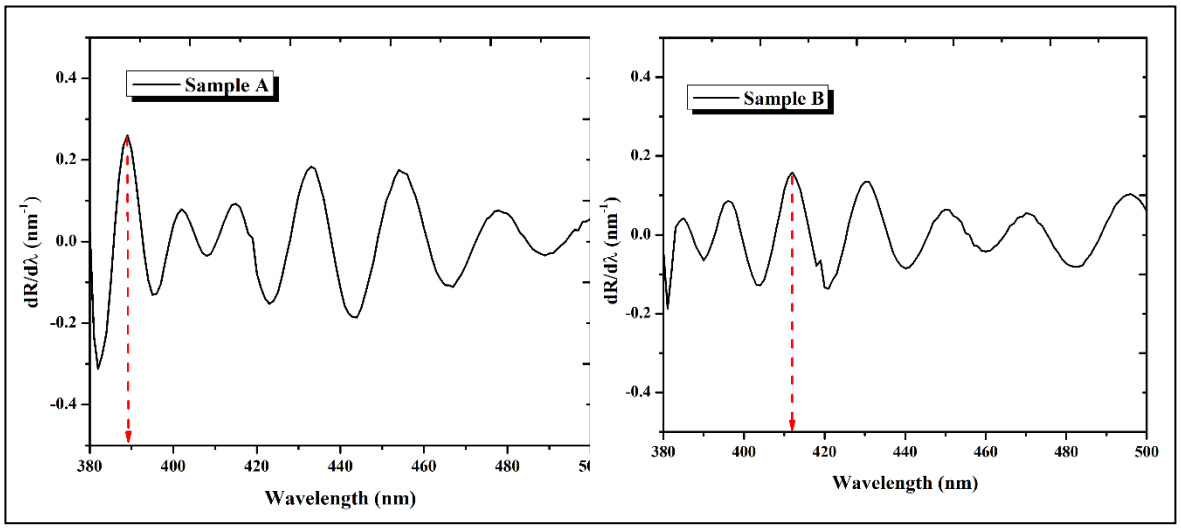

Figure 6. *dR/dλ vs wavelength plots for samples A and B*

4. CONCLUSION

In this work, an AlGaN/GaN/Al_2O_3 HEMT device is investigated. The structure was grown using the MOCVD technique. The main objective of this study is to provide a detailed optical characterization of the investigated samples and to contribute to the existing literature.

The Swanepoel envelope method is applied to the transmission spectra. For Sample A, the refractive index values for the transparent and low-absorption regions are determined to be 1.30 and 2.30, respectively. For the same sample, the absorption and extinction coefficients are found to be 9.7×10^{-3} and 1.1×10^{-3}, respectively. For Sample B, the corresponding values are obtained as 1.40, 2.25, 9.6×10^{-3}, and 1.0×10^{-3}, respectively. The remaining results are presented in Table 2.

In addition, the forbidden energy band gap of AlGaN is determined using the Tauc method and, partially, the Kubelka–Munk method. The forbidden energy band gap values obtained from both methods are approximately 3 eV. These results are in good agreement with those reported in previous studies conducted by different researchers. The relevant references are provided throughout the text.

AUTHOR CONTRIBUTIONS

Ahmet Kürşat Bilgili, wrote the manuscript. Yunus Baş, draw the plots. Orkun Sarıarslan, made the calculations. Sabit Korcak and Mustafa Kemal Öztürk maintained device support and edited the manuscript. All data are available upon request from authors.

AI Exclusion: AI tools are strictly prohibited from being listed as authors.

ACKNOWLEDGEMENT

This study is supported by the Presidency Strategy and Budget Directorate (Grants Numbers: 2016K121220)

CONFLICT OF INTEREST

The authors declare no conflict of interest.

REFERENCES

Alcaraz de la Osa, R., Iparragirre, I., Ortiz, D., & Saiz, J. M. (2019). The extended Kubelka–Munk theory and its application to spectroscopy. *ChemTexts*, *6*(1), 2. https://doi.org/10.1007/s40828-019-0097-0

Dolgonos, A., Mason, T. O., & Poeppelmeier, K. R. (2016). Direct optical band gap measurement in polycrystalline semiconductors: A critical look at the Tauc method. *Journal of Solid State Chemistry*, *240*, 43-48. https://doi.org/10.1016/j.jssc.2016.05.010

Beeler, M., Trichas, E., & Monroy, E. (2013). III-nitride semiconductors for intersubband optoelectronics: a review. *Semiconductor Science and Technology*, *28*(7), 074022. https://doi.org/10.1088/0268-1242/28/7/074022

Bilgili, A. K., Akpınar, Ö., Öztürk, M. K., Başköse, C., Özçelik, S., & Özbay, E. (2019). Investigation of structural, optical and morphological properties of InGaN/GaN structure. *Applied Physics A*, *125*(1), 36. https://doi.org/10.1007/s00339-018-2338-2

Djurisic, A. B., Chan, Y., & Li, E. H. (2001). *Calculations of the refractive index of AlGaN/GaN quantum well*. In: Y. Arakawa, P. Blood, & M. Osinski (Eds.), Proceedings of the Symposium on Integrated Optics (20-26 January 2001, Vol. 4283, p. 630), San Jose, CA, United States. https://doi.org/10.1117/12.432616

Inbaraj, P. F. H., & Prince, J. J. (2017). Optical and structural properties of Mg doped ZnO thin films by chemical bath deposition method. *Journal of Materials Science: Materials in Electronics*, *29*(2), 935-943. https://doi.org/10.1007/s10854-017-7991-2

Mohammad, S. N., & Morkoç, H. (1996). Progress and prospects of group-III nitride semiconductors. *Progress in Quantum Electronics*, *20*(5-6), 361-525. https://doi.org/10.1016/s0079-6727(96)00002-x

Onuma, T., Chichibu, SF., Uchinuma, Y., Sota, T., Yamaguchi, S., Kamiyama, S., Amano, H., & Akasaki, I. (2003). Recombination dynamics of localized excitons in $Al_{1-x}InxN$ epitaxial films on GaN templates grown by metalorganic vapor phase epitaxy. *Journal of Applied Physics*, *94*(4), 2449-2453. https://doi.org/10.1063/1.1592868

Pengelly, R. S., Wood, S. M., Milligan, J. W., Sheppard, S. T., & Pribble, W. L. (2012). A Review of GaN on SiC High Electron-Mobility Power Transistors and MMICs. *IEEE Transactions on Microwave Theory and Techniques*, *60*(6), 1764-1783. https://doi.org/10.1109/tmtt.2012.2187535

Rajan, S., Waltereit, P., Poblenz, C., Heikman, S. J., Green, D. S., Speck, J. S., & Mishra, U. K. (2004). Power Performance of AlGaN–GaN HEMTs Grown on SiC by Plasma-Assisted MBE. *IEEE Electron Device Letters*, *25*(5), 247-249. https://doi.org/10.1109/led.2004.826977

Redko, R., Milenin, G., Milenin, V., Konakova, R., Redko, S., Lytvyn, P., & Babenko, O. (2019). Modification of GaN thin film on sapphire substrate optical properties under weak magnetic fields. *Materials Research Express*, *6*(3), 036413. https://doi.org/10.1088/2053-1591/aaf612

Romanov, I. S., Prudaev, I. A., Brudnyi, V. N., Kopyev, V. V., Novikov, Vad. A., Marmalyuk, A. A., Kureshov, V. A., Sabitov, D. R., & Mazalov, A. V. (2015). Effect of the Barrier Thickness on the Optical Properties of InGaN/GaN/Al_2O_3 (0001) LED Heterostructures. *Russian Physics Journal*, *58*(7), 996-1000. https://doi.org/10.1007/s11182-015-0600-z

Sakalauskas, E., Behmenburg, H., Hums, C., Schley, P., Rossbach, G., Giesen, C., Heuken, M., Kalisch, H., Jansen, R. H., Bläsing, J., Dadgar, A., Krost, A., & Goldhahn, R. (2010). Dielectric function and optical properties of Al-rich AlInN alloys pseudomorphically grown on GaN. *Journal of Physics D: Applied Physics*, *43*(36), 365102. https://doi.org/10.1088/0022-3727/43/36/365102

Swanepoel, R. (1983). Determination of the thickness and optical constants of amorphous silicon. *Journal of Physics E: Scientific Instruments*, *16*(12), 1214-1222. https://doi.org/10.1088/0022-3735/16/12/023